ORIGINAL PAPER

Dipeptidyl peptidase-IV inhibitory activity of dimeric dihydrochalcone glycosides from flowers of *Helichrysum arenarium*

Toshio Morikawa[1,2] · Kiyofumi Ninomiya[1,2] · Junji Akaki[1] · Namiko Kakihara[1] ·
Hiroyuki Kuramoto[1] · Yurie Matsumoto[1] · Takao Hayakawa[1] · Osamu Muraoka[1,2] ·
Li-Bo Wang[3,4] · Li-Jun Wu[4] · Seikou Nakamura[3] · Masayuki Yoshikawa[3] ·
Hisashi Matsuda[3]

Abstract A methanol extract of everlasting flowers of *Helichrysum arenarium* L. Moench (Asteraceae) was found to inhibit the increase in blood glucose elevation in sucrose-loaded mice at 500 mg/kg p.o. The methanol extract also inhibited the enzymatic activity against dipeptidyl peptidase-IV (DPP-IV, $IC_{50} = 41.2$ μg/ml), but did not show intestinal α-glucosidase inhibitory activities. From the extract, three new dimeric dihydrochalcone glycosides, arenariumosides V–VII (**2–4**), were isolated, and the stereostructures were elucidated based on their spectroscopic properties and chemical evidence. Of the constituents, several flavonoid constituents, including **2–4**, were isolated, and these isolated constituents were investigated for their DPP-IV inhibitory effects. Among them, chalconaringenin 2′-*O*-β-D-glucopyranoside (**16**, $IC_{50} = 23.1$ μM) and aureusidin 6-*O*-β-D-glucopyranoside (**35**, 24.3 μM) showed relatively strong inhibitory activities.

Introduction

An Asteraceae plant, *Helichrysum arenarium* L. Moench (common names "dwarf everlasting" or "immortelle"), has an extensive distribution throughout Europe. The choleretic, hepatoprotective, and detoxifying activities of the inflorescence of this plant are known to European folk medicine [1]. The extract from the inflorescence of this plant has been characterized as showing free-radical scavenging actions [1] and antibacterial activities against lower respiratory tract pathogens [2]. Several flavonoids, megastigmanes, α-pyrones, and phthalides have been isolated from the flowers [3–9], achenes [10], roots [11, 12], capitula, and leafy stems [13] of *H. arenarium*. In the course of our studies on bioactive constituents from the flowers of *H. arenarium* [4–6], we have reported that the methanol extract and several flavonoids showed inhibitory effects on tumor necrosis factor-α (TNF-α)-induced cytotoxicity in L929 cells [4]. We further evaluated the extract and its constituents and found that the methanol extract inhibited blood glucose elevation in sucrose-loaded mice. A serine protease dipeptidyl peptidase-IV (DPP-IV) is widely expressed in the endothelial cells throughout the body and is found in a circulating soluble form [14]. It has been shown that the incretin hormone glucagon-like peptide-1 (GLP-1) is released from the intestinal L-cells into the circulation in response to the ingestion of food and stimulates both insulin biosynthesis and secretion [15, 16]. Apart from several other beneficial effects, GLP-1 regulates insulin in a strictly glucose-dependent manner, and inhibition of the enzyme DPP-IV, which rapidly inactivates

✉ Toshio Morikawa
morikawa@kindai.ac.jp

✉ Hisashi Matsuda
matsuda@mb.kyoto-phu.ac.jp

1 Pharmaceutical Research and Technology Institute, Kinki University, 3-4-1 Kowakae, Higashi-osaka, Osaka 577-8502, Japan

2 Antiaging Center, Kinki University, 3-4-1 Kowakae, Higashi-osaka, Osaka 577-8502, Japan

3 Kyoto Pharmaceutical University, Misasagi, Yamashina-ku, Kyoto 607-8412, Japan

4 Faculty of Natural Medicines, Shenyang Pharmaceutical University, 103 Wenhua Rd., 110016 Shenyang, People's Republic of China

GLP-1, has been shown to increase the half-life of GLP-1 and to prolong the effects of this incretin hormone. The human recombinant DPP-IV inhibitory activity was revealed to regulate the antidiabetic effect of the extract. Further separation of the active constituents in the extract allowed us to isolate a known and novel new dimeric dihydrochalcone glycosides, tomoroside A (**1**) [17] and arenarumosides V–VII (**2–4**), respecitvely. Here, we describe the isolation and elucidation of the structure of **2–4** as well as the DPP-IV inhibitory activity of the flavonoid constituents (**1–34**).

Results and discussion

Effects of the methanol extract on plasma glucose levels in sucrose-loaded mice

Dried flowers of *H. arenarium* were extracted with methanol under reflux to yield a methanol extract (19.8 % from the dried material). As shown in Table 1, the methanol extract showed an inhibitory effect against the increase in blood glucose levels in sucrose-loaded mice at a dose of 500 mg/kg, p.o.

Effects of the methanol extract and its fractions on human recombinant DPP-IV activity

To characterize the mode of action of the antihyperglycemic effect of the methanol extract, in vitro inhibitory activities on enzymes such as rat small intestinal α-glucosidases, maltase, and sucrose, and human recombinant DPP-IV inhibitory activities were examined. As shown in Table 2, the methanol extract was found to show an inhibitory effect on DPP-IV ($IC_{50} = 41.2$ μg/ml), but did not show α-glucosidase inhibitory activities (both $IC_{50} > 300$ μg/ml). Following this, the methanol extract was partitioned with EtOAc–H_2O (1:1, v/v) to furnish an EtOAc-soluble fraction (0.58 %) and an aqueous phase. The aqueous phase was subjected to Diaion HP-20 column chromatography ($H_2O \rightarrow$ MeOH) to yield H_2O- and MeOH-eluted fractions (21.5 and 0.73 %, respectively). A bioassay-guided fractionation revealed that the EtOAc-soluble and MeOH-eluted fractions showed DPP-IV inhibitory activities ($IC_{50} = 16.0$ and 25.4 μg/ml, respectively), whereas the H_2O-eluted fraction showed no notable activity ($IC_{50} = 273$ μg/ml).

Table 1 Inhibitory effect of the methanol extract on plasma glucose levels in sucrose-loaded mice

Treatment	Dose (mg/kg, p.o.)	N	Blood glucose (mg/dl)[a]		
			0.5 h	1 h	2 h
Normal	–	7	126.3 ± 20.2^c	115.3 ± 10.6^c	99.3 ± 11.7^c
Control	–	12	279.5 ± 10.0	254.7 ± 10.9	172.8 ± 8.4
MeOH extract	500	7	236.8 ± 10.7^c	257.5 ± 9.2	182.6 ± 5.0
	1000	7	193.3 ± 10.6^c	214.1 ± 5.1^c	180.8 ± 4.7
	2000	7	179.7 ± 3.6^c	199.5 ± 4.4^c	178.3 ± 5.6
Normal	–	6	124.8 ± 7.3^c	143.0 ± 5.4^c	131.8 ± 6.4^c
Control	–	9	218.7 ± 4.0	208.9 ± 6.8	163.7 ± 3.7
Acarbose [32]	10	6	162.4 ± 11.7^c	183.8 ± 3.8^b	151.5 ± 6.3
	20	6	153.8 ± 10.2^c	185.4 ± 8.1^b	152.8 ± 3.8

[a] Values represent the mean $\pm$ SEM

Significantly different from the control group, [b] $p < 0.05$, [c] $p < 0.01$

Table 2 Inhibitory effects of the methanol extract and its fractions on rat small intestinal α-glucosidases and human recombinant DPP-IV activity

	Rat α-glucosidase IC_{50} (μg/ml)[a]		DPP-IV
	Maltase	Sucrase	IC_{50} (μg/ml)[a]
MeOH extract	>300 (28.2)[b]	>300 (32.0)[b]	41.2
EtOAc-soluble fraction	271	>300 (46.6)[b]	16.0
MeOH-eluted fraction	>300 (46.2)[b]	>300 (43.3)[b]	25.4
H_2O-eluted fraction	>300 (10.2)[b]	>300 (7.1)[b]	273

[a] Each value represents the mean of 2–4 experiments

Values in parentheses present inhibition % at [b] 300 μM (for α-glucosidases)

Isolation

In the present study, we additionally isolated four dimeric dihydrochalcone glycosides, tomoriside A (**1**, 1.09 %) [17] and arenariumosides V (**2**, 0.0030 %), VI (**3**, 0.010 %), and VII (**4**, 0.018 %) from the MeOH-eluted fraction (Fig. 1) and (2*R*)-helichrysin A (**9**, 0.12 %), (2*S*)-helichrysin A (**10**, 0.037 %), chalconeringenin 2′-*O*-β-D-glucopyranoside (**16**, 0.11 %), apigenin 7-*O*-β-D-glucopyranoside (**18**, 0.045 %), kaempferol 7-*O*-β-D-glucopyranoside (**27**, 0.39 %), and quercetin 3-*O*-β-D-glucopyranoside (**32**, 0.027 %) from the EtOAc-soluble fraction using normal-phase silica gel and reversed-phase ODS column chromatography, and finally HPLC.

Structural identification and determination of dimeric dihydrochalcone glycosides (1–4)

In the positive-ion fast atom bombardment (FAB) MS spectrum of **1**, a quasimolecular ion peak was observed at *m/z* 891 [M+Na]$^+$, and HRFABMS analysis revealed the molecular formula to be $C_{42}H_{44}O_{20}$. The ^1H and ^{13}C NMR (pyridine-d_5 at 40 °C with TMS as an internal standard) spectroscopic properties of **1** were in accordance with those of reported data [17] except for the deviations of the chemical shift, as shown in Table 3 ($\Delta\delta_H$: from 0 to 0.08 ppm; $\Delta\delta_C$: from 0.6 to 1.3 ppm). The ^1H and ^{13}C NMR spectra (pyridine-d_5) of **1**, which were assigned with the aid of DEPT, ^1H-^1H COSY, HMQC, and HMBC experiments, showed signals assignable to four methines [δ 5.56 (1H, dd, *J* = 5.8, 10.3 Hz, H-α′), 5.97 (1H, dd, *J* = 8.7, 10.9 Hz, H-α), 6.06 (1H, dd, *J* = 5.8, 10.9 Hz H-β′), 6.11 (1H, dd, *J* = 8.7, 10.3 Hz, H-β)], two pairs of ABX type 1,2,4,6-tetrasubstituted aromatic protons [δ 6.25, 6.70 (1H each, both d, *J* = 2.2 Hz, H-5‴,3‴), 6.25, 6.74 (1H each, both d, *J* = 2.2 Hz, H-5′,3′)], and two pairs of A$_2$B$_2$ type 1,4-disubstituted aromatic protons [δ 6.84, 7.90 (2H each, both d, *J* = 8.7 Hz, H-3″,5″, 2″,6″), 6.93, 8.10 (2H each, both d, *J* = 8.7 Hz, H-3,5, 2,6)] together with two glucopyranosyl units [δ 5.70 (1H, d, *J* = 8.0 Hz, 2′-*O*-Glc-H-1‴‴), 5.87 (1H, d, *J* = 8.0 Hz, 2‴-*O*-Glc-H-1‴‴‴)].

As shown in Fig. 2, the ^1H-^1H COSY experiment on **1** indicated the presence of partial structures written in bold lines. In an HMBC experiment, long-range correlations were observed between H-α and C-1 (δ_C 131.2), H-β and C-7′ (δ_C 203.8), H-α′ and C-1″ (δ_C 131.6), H-β′ and C-7‴ (δ_C 204.8), 2′-*O*-Glc-H-1‴‴ and C-2′ (δ_C 161.4), and 2‴-*O*-Glc-H-1‴‴‴ and C-2‴ (δ_C 160.9). The stereochemistry of **1** was characterized by the rotating frame nuclear Overhauser effect spectroscopy (ROESY) experiment, which showed the rotating frame nuclear Overhauser effect (ROE) correlations between H-β and H-α′/H$_2$-2,6 as well as H-β′ and H-α/H$_2$-2″,6″ (Fig. 2). Thus, the configuration of the cyclobutane moiety in **1** was determined to be an α-truxillic type structure [18–20]. Based on these findings, the structure of **1** was identified to be tomoroside A.

Arenariumoside V (**2**) was obtained as a yellow powder with positive optical rotation ([α]$_D^{27}$ +32.1 in MeOH). The IR spectrum showed absorption bands at 1619 cm^{-1} (carbonyl), 1509 and 1458 cm^{-1} (aromatic ring) and broad bands at 3568 and 1074 cm^{-1}, suggestive of a glycosyl moiety. In the positive ion FABMS, a quasimolecular ion

Fig. 1 Dimeric dihydrochalcone glycosides (1–4) from the flowers of *H. arenarium*
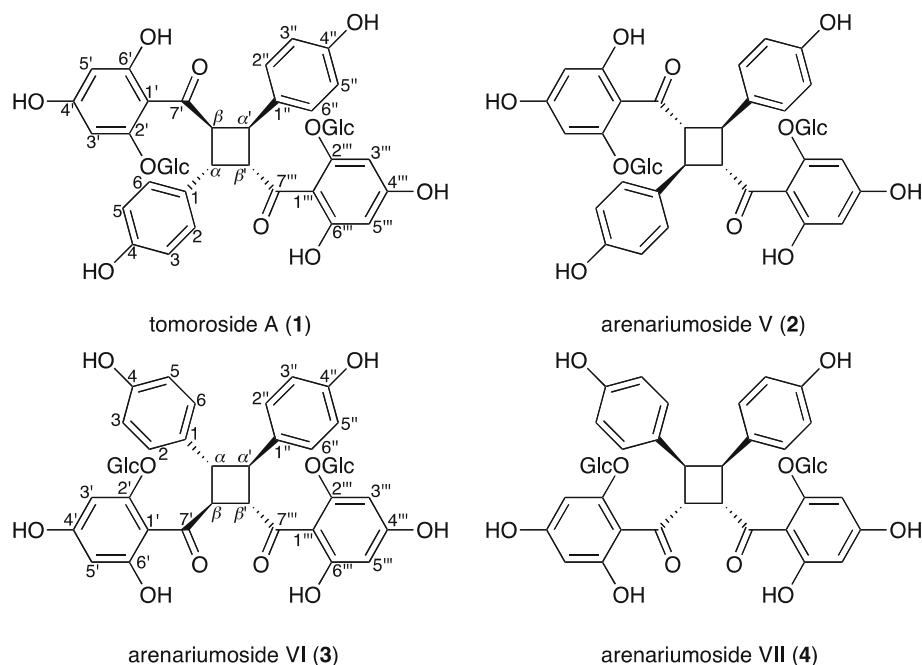
tomoroside A (**1**)

arenariumoside V (**2**)

arenariumoside VI (**3**)

arenariumoside VII (**4**)

Table 3 ^{1}H (500 MHz) and ^{13}C NMR (125 MHz) data of tomoroside A (**1**)

Position	**1**^{a}		**1**^{b}		$\Delta\delta_H$	$\Delta\delta_C$
	δ_H (*J*, Hz)	δ_C	δ_H (*J*, Hz)	δ_C	δ_H**1**$^{b-a}$	δ_C**1**$^{b-a}$
1		131.2		132.1		0.9
2,6	8.10 (2H, d, 8.7)	129.8	8.15 (2H, d, 8.6)	130.9	0.05	1.1
3,5	6.93 (2H, d, 8.7)	115.2	6.97 (2H, d, 8.6)	116.0	0.04	0.8
4		156.5		157.5		1.0
4-OH			10.90 (br s)			
α	5.97 (dd, 8.7, 10.9)	41.6	6.02 (dd, 8.3, 11.1)	42.6	0.05	1.0
β	6.11 (dd, 8.7, 10.3)	53.4	6.15 (dd, 8.3, 10.5)	54.3	0.04	0.9
1′		106.0		106.9		0.9
2′		161.4		162.4		1.0
3′	6.74 (d, 2.2)	94.5	6.78 (d, 2.2)	95.6	0.04	1.1
4′		165.5		166.7		1.2
4′-OH			12.68 (br s)			
5′	6.25 (d, 2.2)	97.3	6.28 (d, 2.2)	98.3	0.03	1.0
6′		167.1		168.1		1.0
6′-OH	14.47 (br s)		14.55 (s)		0.08	
7′		203.8		204.9		1.1
1″		131.6		132.6		1.0
2″, 6″	7.90 (2H, d, 8.7)	129.8	7.92 (2H, d, 8.6)	130.9	0.02	1.1
3″, 5″	6.84 (2H, d, 8.7)	115.4	6.84 (2H, d, 8.6)	116.2	0	0.8
4″		156.5		157.4		0.9
4″-OH			10.83 (br s)			
α′	5.56 (dd, 5.8, 10.3)	41.6	5.60 (dd, 5.5, 10.5)	42.5	0.04	0.9
β′	6.06 (dd, 5.8, 10.9)	54.6	6.08 (dd, 5.5, 11.1)	55.8	0.02	1.2
1‴		106.8		107.7		0.9
2‴		160.9		161.9		1.0
3‴	6.70 (d, 2.2)	94.8	6.74 (d, 2.2)	95.7	0.04	0.9
4‴		165.6		166.9		1.3
4‴-OH			12.68 (br s)			
5‴	6.25 (d, 2.2)	97.3	6.27 (d, 2.2)	98.3	0.02	1.0
6‴		167.2		168.2		1.0
6‴-OH	14.47 (br s)		14.59 (s)		0.12	
7‴		204.8		205.7		0.9
2′-*O*-Glc						
Glc-1⁗	5.70 (d, 8.0)	101.8	5.74 (d, 7.8)	102.8	0.04	1.0
Glc-2⁗	5.10 (dd, 8.0, 9.0)	74.5	5.16 (t, 8.2)	75.6	0.06	1.1
Glc-3⁗	4.31 (m)	78.5	4.34 (m)	79.4	0.03	0.9
Glc-4⁗	4.40 (m)	70.8	4.43 (m)	71.7	0.03	0.9
Glc-5⁗	3.99 (m)	79.0	4.02 (ddd, 2.4, 5.4, 8.0)	79.7	0.03	0.7
Glc-6⁗	4.33 (m)	61.9	4.36 (m)	62.7	0.03	0.8
	4.40 (m)		4.43 (m)		0.03	
2‴-*O*-Glc						
Glc-1‴″	5.87 (d, 8.0)	100.7	5.92 (d, 7.8)	101.5	0.05	0.8
Glc-2‴″	4.77 (dd, 8.0, 8.9)	74.2	4.81 (t, 8.2)	75.2	0.04	1.0
Glc-3‴″	4.34 (m)	78.6	4.38 (m)	79.8	0.04	1.2
Glc-4‴″	4.32 (m)	70.5	4.36 (m)	71.4	0.04	0.9
Glc-5‴″	3.91 (m)	79.0	3.95 (ddd, 2.3, 5.3, 7.8)	79.6	0.04	0.6

Table 3 continued

Position	1[a]		1[b]		$\Delta\delta_H$	$\Delta\delta_C$
	δ_H (J, Hz)	δ_C	δ_H (J, Hz)	δ_C	δ_H 1[b–a]	δ_C 1[b–a]
Glc-6′′′′′	4.23 (m)	61.7	4.27 (dd, 5.2, 12)	62.6	0.04	0.9
	4.32 (m)		4.37 (m)		0.05	

[a] Measured in pyridine-d_5 at 40 °C (tetramethylsilane as an internal standard)

[b] Measured in pyridine-d_5 [17]

peak was observed at m/z 891 [M+Na]⁺, and HRFABMS analysis revealed the molecular formula to be $C_{42}H_{44}O_{20}$, which was the same as that of **1**. Acid hydrolysis of **2** with 1 M hydrochloric acid (HCl) liberated D-glucose, which was identified by HPLC analysis [21, 22]. The ¹H and ¹³C NMR spectra of **2** (pyridine-d_5, Table 4) showed signals assignable to a cyclobutane moiety [δ 5.66 (1H, dd, J = 9.6, 10.4 Hz, H-β), 5.95 (1H, dd, J = 9.6, 10.4 Hz, H-α), 5.96 (1H, dd, J = 9.6, 9.6 Hz H-β′), 6.16 (1H, dd, J = 9.6, 9.6 Hz, H-α′)], 12 aromatic protons {two pairs of ABX type 1,2,4,6-tetrasubstituted aromatic protons [δ 6.21, 6.68 (1H each, both d, J = 2.4 Hz, H-5′′′,3′′′), 6.24, 6.65 (1H each, both d, J = 2.4 Hz, H-5′,3′)] and two pairs of A_2B_2 type 1,4-disubstituted aromatic protons [δ 6.74, 7.82 (2H each, both br d, J = ca. 8 Hz, H-3′′,5′′, 2′′,6′′), 7.04, 7.86 (2H each, both br d, J = ca. 9 Hz, H-3,5, 2,6)], and two glucopyranosyl units [δ 5.55 (1H, d, J = 8.0 Hz, 2′-O-Glc-H-1′′′′), 5.80 (1H, d, J = 8.0 Hz, 2′′′-O-Glc-H-1′′′′′)]. The ¹H and ¹³C NMR spectroscopic properties of **2** were quite similar to those of **1**. The ¹H-¹H COSY experiment on **2** indicated the presence of a partial structure shown in bold lines as shown in Fig. 2. The connectivities of the

hydroxyl and carbonyl moieties as well as the glucopyranosyl parts in **2** were characterized on the basis of the HMBC experiment, in which long-range correlations were observed between H-α and C-1 (δ_C 136.2), H-β and C-7′ (δ_C 204.5), H-α′ and C-1′′ (δ_C 130.2), H-β′ and C-7′′′ (δ_C 204.6), 2′-O-Glc-H-1′′′′ and C-2′ (δ_C 162.6), and 2′′′-O-Glc-H-1′′′′′ and C-2′′′ (δ_C 161.2). In the ROESY experiment, the ROE correlations were observed between H-β and H₂-2,6/H₂-2′′,6′′ and H-β′ and H₂-2,6/H₂-2′′,6′′ (Fig. 2). Consequently, the stereochemistry of the cyclobutane moiety in **2** was determined to be an ε-truxillic type structure.

Arenariumosides VI (**3**) and VII (**4**), $C_{42}H_{44}O_{20}$, were also obtained as a yellow powders with negative and positive optical rotations (**3**: $[\alpha]_D^{26}$ −16.7; **4**: $[\alpha]_D^{27}$ +6.0 both in MeOH). The acid hydrolysis of **3** and **4** liberated D-glucose, respectively. The proton and carbon signals in the ¹H and ¹³C NMR (pyridine-d_5, Table 4) spectra of **3** and **4** were superimposable on those of **2** and indicated the presence of the same functional groups: a cyclobutane moiety [**3**: δ 4.30, 5.96 (2H each, both br d, J = ca. 9 Hz, H-α,α′, H-β,β′); **4**: δ 4.41 (1H, dd, J = 5.4, 9.6 Hz, H-α),

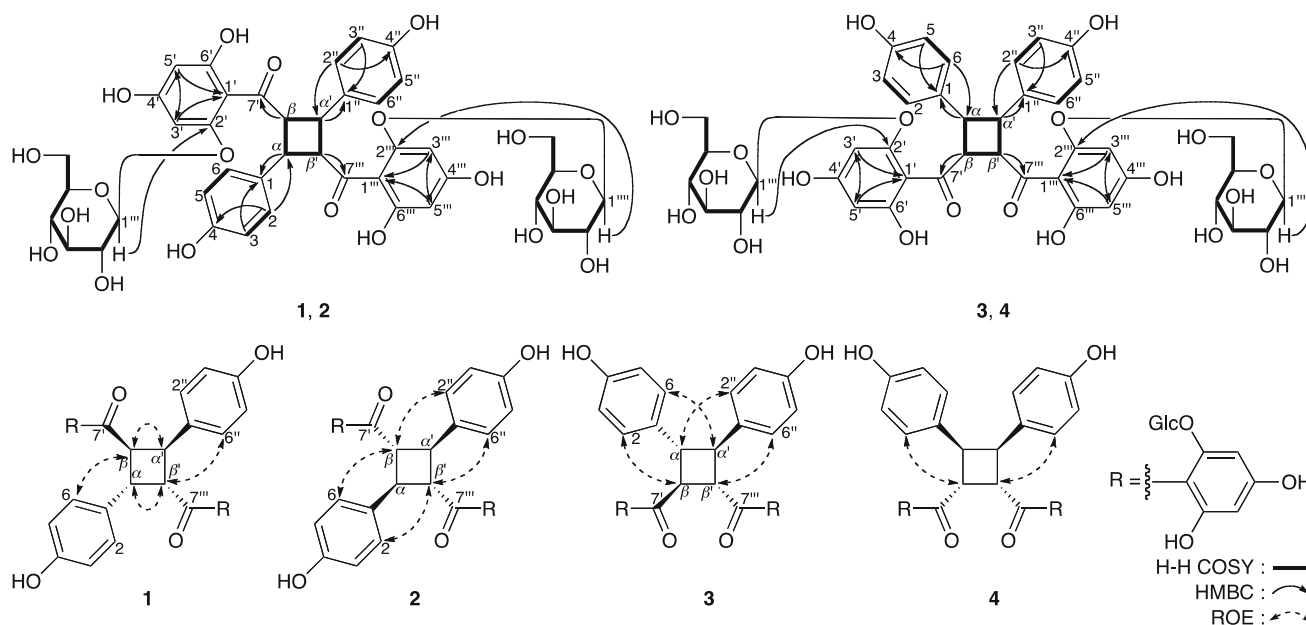**Fig. 2** ¹H-¹H COSY, HMBC, and ROE correlations of **1**–**4**

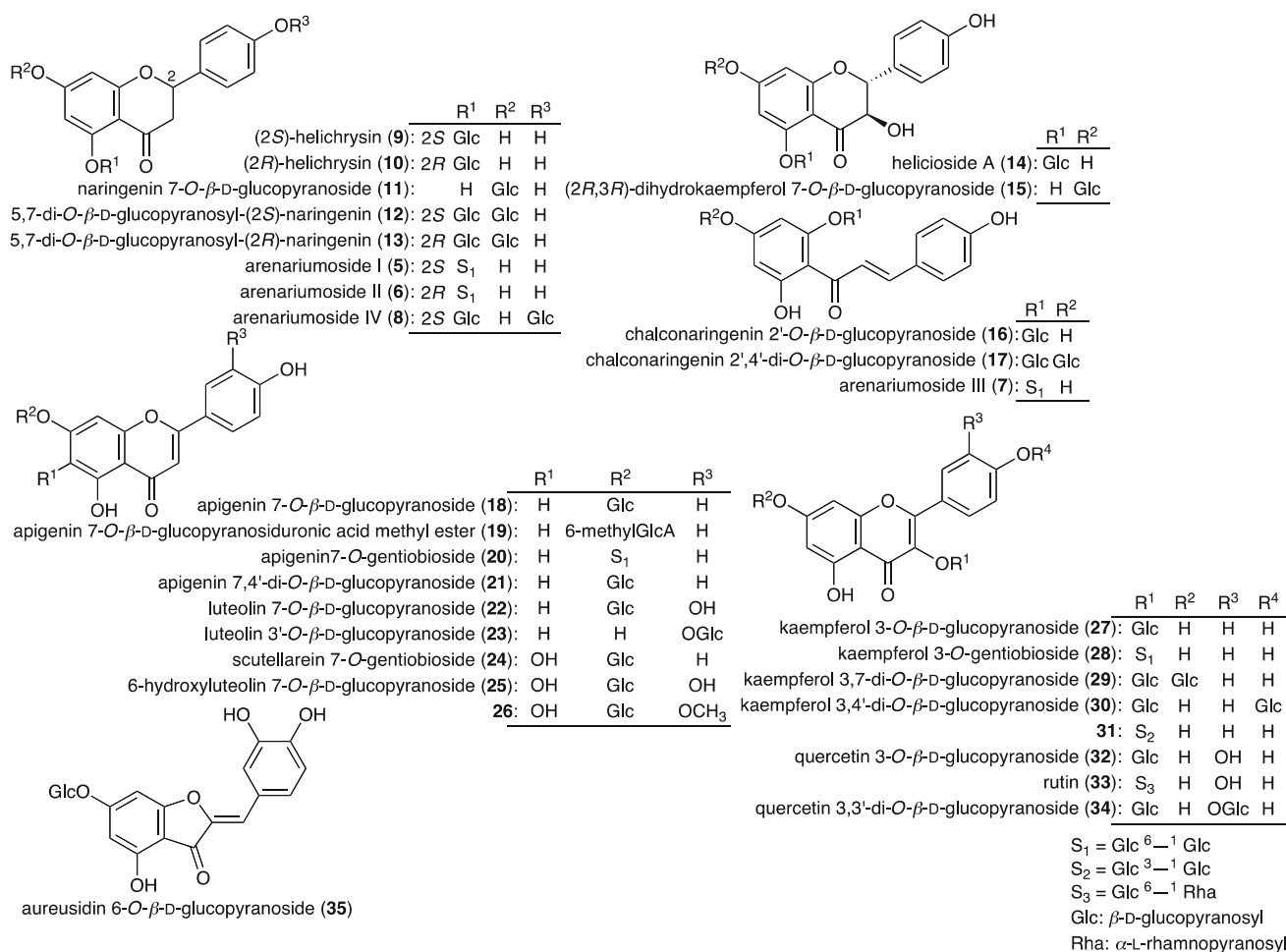**Fig. 3** Flavonoids (**5–34**) from the flowers of *H. arenarium*

5.04 (1H, dd, $J = 9.2$, 9.6 Hz, H-α'), 6.01 (1H, dd, $J = 9.2$, 9.2 Hz H-β'), 6.12 (1H, dd, $J = 5.4$, 9.2 Hz, H-β')], two pairs of ABX type 1,2,4,6-tetrasubstituted aromatic protons [**3**: δ 6.38, 6.65 (2H each, both d, $J = 1.9$ Hz, H-5′,5‴, 3′,3‴); **4**: δ 6.45, 6.65 (1H each, both d, $J = 2.3$ Hz, H-5′,3′), 6.55, 6.85 (1H each, both d, $J = 2.3$ Hz, H-5‴,3‴)], two pairs of A_2B_2 type 1,4-disubstituted aromatic protons [**3**: δ 7.08, 7.59 (4H each, both br d, $J =$ ca. 8 Hz, H-3,5,3″,5″, 2,6,2″,6″); **4**: δ 6.94, 7.40 (2H each, both d, $J = 8.4$ Hz, H-3″,5″, 2″,6″), 7.08, 7.63 (2H each, both d, $J = 8.4$ Hz, H-3,5, 2,6)], and two glucopyranosyl units [**3**: δ 5.50 (2H, d, $J = 7.7$ Hz, 2′-*O*-Glc-H-1⁗, 2‴-*O*-Glc-H-1″″′); **4**: δ 5.35 (1H, d, $J = 7.7$ Hz, 2‴-*O*-Glc-H-1″″′), 5.53 (1H, d, $J = 8.0$ Hz, 2′-*O*-Glc-H-1⁗)]. The head-to-head conjugated dimeric dihydrochalcone structures of **3** and **4** were determined on the basis of the ¹H-¹H COSY and HMBC experiments (Fig. 2). The ROE correlations in the ROESY experiments of **3** and **4** were observed as shown in Fig. 2; the stereochemistry of the cyclobutane moieties in **3** and **4**

were elucidated to be δ- and β-truxinic type structures, respectively.

To our knowledge, dimeric dihydrocalcones isolated from natural resources are rare, and the first report of a dimeric dihydrochalcone, brackenin, which was isolated from *Brackenridgea zanguebarica*, was established in 1983 [23]. A few other dimeric dihydrochalcones have been reported [24–30]. Recently, a dimeric dihydrochalcone glycoside, tomoroside A (**1**), was isolated from the same genus *Helichysum zivojinii* [17]. This article is the second report on the isolation and structural determination of dimeric dihydrochalcone glycosides from the genus *Helichrysum*.

Effects of the flavonoid constituents on human recombinant DPP-IV activity

In order to specify the principal active constituents, the inhibitory effects of the isolates from the active fractions described above (the EtOAc-soluble and the MeOH-eluted

Table 4 ^{1}H (500 MHz) and ^{13}C NMR (125 MHz) data of arenariumosides V–VII (**2–4**)

Position	2[a] δ_H (J, Hz)	δ_C	2[b] δ_H (J, Hz)	δ_C	3[a] δ_H (J, Hz)	δ_C	4[a] δ_H (J, Hz)	δ_C
1		136.2		134.2		133.7		132.7
2, 6	7.86 (2H, br d, ca. 9)	129.4	7.12 (2H, br d, ca. 8)	128.0	7.59 (2H, br d, ca. 8)	129.3	7.63 (2H, d, 8.4)	130.9
3, 5	7.04 (2H, br d, ca. 9)	116.2	6.65 (2H, br d, ca. 8)	114.7	7.08 (2H, br d, ca. 8)	116.3	7.08 (2H, d, 8.4)	115.8
4		157.1		154.8		157.7		157.0
α	5.95 (dd, 9.6, 10.4)	48.8	4.83 (dd, 9.4, 10.1)	46.9	4.30 (br d, ca. 9)	48.1	4.41 (dd, 5.4, 9.6)	47.8
β	5.66 (dd, 9.6, 10.4)	56.2	4.70 (m)	54.1	5.96 (br d, ca. 9)	52.5	6.12 (dd, 5,4, 9.2)	58.1
1′		106.8		105.1		107.8		105.7
2′		162.6		161.2		161.1		162.2
3′	6.65 (d, 2,4)	95.7	6.04 (br s)	94.4	6.65 (d, 1.9)	96.5	6.65 (d, 2.3)	96.1
4′		167.5		163.8		165.9		166.1
5′	6.24 (d, 2.4)	98.2	5.72 (br s)	96.5	6.38 (d, 1.9)	98.3	6.45 (d, 2.3)	98.5
6′		167.9		165.6		166.1		167.6
6′-OH	14.88 (s)				13.73 (s)		14.10 (br s)	
7′		204.5		203.2		204.8		204.8
1″		130.2		128.5		133.7		132.1
2″, 6″	7.82 (2H, br d, ca. 8)	131.6	6.84 (2H, br d, ca. 8)	129.3	7.59 (2H, br d, ca. 8)	129.3	7.40 (2H, d, 8.4)	130.0
3″, 5″	6.74 (2H, br d, ca. 8)	115.4	6.24 (2H, br d, ca. 8)	113.8	7.08 (2H, br d, ca. 8)	116.3	6.94 (2H, d, 8.4)	115.6
4″		157.0		155.3		157.7		156.6
α′	6.16 (dd, 9.6, 9.6)	37.8	4.99 (m)	36.3	4.30 (br d, ca. 9)	48.1	5.04 (dd, 9.2, 9.6)	43.4
β′	5.96 (dd, 9.6, 9.6)	55.5	4.92 (dd, 9.4, 9.7)	53.8	5.96 (br d, ca. 9)	52.5	6.01 (dd, 9.2, 9.2)	52.8
1‴		107.9		106.5		107.8		107.1
2‴		161.2		159.7		161.1		161.8
3‴	6.68 (d, 2.4)	96.7	6.04 (br s)	95.9	6.65 (d, 1.9)	96.5	6.85 (d, 2.3)	96.1
4‴		166.3		164.4		165.9		166.9
5‴	6.21 (d, 2.4)	98.5	5.70 (br s)	96.9	6.38 (d, 1.9)	98.3	6.55 (d, 2.3)	98.6
6‴		167.9		165.2		166.1		166.9
6‴-OH	14.42 (s)				13.73 (s)		14.49 (br s)	
7‴		204.6		203.3		204.8		205.8
2′-O-Glc								
Glc-1⁗	5.55 (d, 8.0)	103.5	4.79 (d, 7.9)	101.9	5.50 (d, 7.7)	102.5	5.53 (d, 8.0)	104.1
Glc-2⁗	5.19 (dd, 8.0, 8.8)	74.5	3.42 (m)	73.6	4.38 (m)	74.5	4.71 (dd, 8.0, 8.8)	74.0
Glc-3⁗	3.92 (m)	79.2	3.92 (m)	77.0	3.86 (m)	79.0	3.73 (m)	78.9
Glc-4⁗	4.16 (m)	71.2	3.27 (m)	69.7	4.22 (m)	71.3	4.47 (dd, 8.8, 9.0)	70.9
Glc-5⁗	3.92 (m)	79.8	3.31 (m)	77.5	3.83 (m)	79.0	4.20 (m)	79.3
Glc-6⁗	4.12 (m)	62.4	3.59 (dd, 5.2, 12.2)	60.8	4.22 (m)	62.6	4.22 (m)	62.1
	4.30 (m)		3.82 (m)		4.33 (m)		4.28 (m)	
2‴-O-Glc								
Glc-1⁗′	5.80 (d, 8.0)	102.4	5.05 (d, 7.6)	100.9	5.50 (d, 7.7)	102.5	5.35 (d, 7.7)	102.8
Glc-2⁗′	4.63 (dd, 8.0, 8.8)	74.1	3.42 (m)	73.5	4.38 (m)	74.5	3.63 (dd, 7.7, 8.5)	73.2
Glc-3⁗′	4.26 (m)	79.4	3.92 (m)	77.0	3.86 (m)	79.0	3.95 (m)	78.5
Glc-4⁗′	4.55 (m)	71.4	3.72 (m)	69.7	4.22 (m)	71.3	3.93 (m)	71.2
Glc-5⁗′	3.92 (m)	79.7	3.26 (m)	77.4	3.83 (m)	79.0	3.83 (m)	79.0
Glc-6⁗′	4.12 (m)	62.4	3.32 (dd, 5.2, 12.2)	60.7	4.22 (m)	62.6	4.12 (m)	62.8
	4.30 (m)		3.67 (m)		4.33 (m)		4.32 (m)	

Measured in [a]pyridine-d$_5$ or [b]DMSO-d$_6$ at 40 °C (tetramethylsilane as an internal standard)

fraction) on human recombinant DPP-IV activity were tested.

In our previous study, we isolated 30 flavonoid constituents from the active MeOH-eluted fraction, including arenariumosides I (5, 0.0045 %), II (6, 0.0059 %), III (7, 0.0046 %), and IV (8, 0.0034 %), (2S)-helichrysin (9, 0.13 %), (2R)-helichrysin (10, 0.0016 %), neringenin 7-O-β-D-glucopyranoside (11, 0.0053 %), 5,7-di-O-β-D-glucopyranosyl-(2S)-naringenin (12, 0.0045 %), 5,7-di-O-β-D-glucopyranosyl-(2R)-naringenin (13, 0.0097 %), helicioside A (14, 0.0015 %), (2R,3R)-dihydrokaempferol 7-O-β-D-glucopyranoside (15, 0.010 %), chalconeringenin 2′-O-β-D-glucopyranoside (16, 0.013 %), chalconeringenin 2′,4′-di-O-β-D-glucopyranoside (17, 0.0060 %), apigenin 7-O-β-D-glucopyranoside (18, 0.0025 %), apigenin 7-O-β-D-glucopyranosiduronic acid methyl ester (19, 0.0024 %), apigenin 7-O-gentiobioside (20, 0.0040 %), apigenin 7,4′-di-O-β-D-glucopyranoside (21, 0.019 %), luteolin 7-O-β-D-glucopyranoside (22, 0.0025 %), luteolin 3′-O-β-D-glucopyranoside (23, 0.0013 %), scutellarein 7-O-gentiobioside (24, 0.0017 %), 6-hydroxyluteolin 7-O-β-D-glucopyranoside (25, 0.020 %), 6-hydroxy-3′-O-methylluteolin 7-O-β-D-glucopyranoside (26, 0.0033 %), kaempferol 7-O-β-D-glucopyranoside (27, 0.58 %), kaempferol 3-O-gentiobioside (28, 0.0070 %), kaempferol 3,7,-di-O-β-D-glucopyranoside (29, 0.0025 %), kaempferol 3,4′-di-O-β-D-glucopyranoside (30, 0.0011 %), kaempferol 3-O-β-D-glucopyranosyl-(1 → 3)-β-D-glucopyranoside (31, 0.0040 %), quercetin 3-O-β-D-glucopyranoside (32, 0.037 %), rutin (33, 0.0032 %), quercetin 3,3′-di-O-β-D-glucopyranoside (34, 0.0015 %), and aureusidin 6-O-β-D-glucopyranoside (35, 0.0025 %), as shown in Fig. 3 [4–6].

As shown in Table 5, we found that the following flavonoids had DPP-IV inhibitory activities: arenariumosides V (2, IC_{50} = 83.0 μM), VI (3, 52.0 μM), VII (4, 83.0 μM), and III (7, 54.1 μM), chalconaringenin 2′-O-β-D-glucopyranoside (16, 23.1 μM), chalconeringenin 2′,4′-di-O-β-D-glucopyranoside (17, 70.0 μM), apigenin 7-O-β-D-glucopyranoside (18, 62.7 μM), apigenin 7-O-β-D-glucopyranosiduronic acid methyl ester (19, 50.5 μM), apigenin 7-O-gentiobioside (20, 32.0 μM), luteolin 7-O-β-D-glucopyranoside (22, 37.5 μM), 6-hydroxyluteolin 7-O-β-D-glucopyranoside (25, 60.3 μM), 6-hydroxy-3′-O-methylluteolin 7-O-β-D-glucopyranoside (26, 73.2 μM), kaempferol 3-O-gentiobioside (28, 58.0 μM), kaempferol 3,7,-di-O-β-D-glucopyranoside (29, 36.8 μM), kaempferol 3,4′-di-O-β-D-glucopyranoside (30, 88.6 μM), kaempferol 3-O-β-D-glucopyranosyl-(1 → 3)-β-D-glucopyranoside (31, 85.2 μM), quercetin 3-O-β-D-glucopyranoside (32, 56.6 μM), quercetin 3,3′-di-O-β-D-glucopyranoside (34, 73.9 μM), and aureusidin 6-O-β-D-glucopyranoside (35, 24.3 μM). Among them, 16 and 35 showed relatively

Table 5 Inhibitory effects of the flavonoid constituents (1–35) on human recombinant DPP-IV activity

	IC_{50} (μM)[a]
Tomoroside A (1)	>100 (46.8)[b]
Arenariumoside V (2)	83.0
Arenariumoside VI (3)	52.0
Arenariumoside VII (4)	83.0
Arenariumoside I (5)	>100 (31.4)[b]
Arenariumoside II (6)	>100 (41.6)[b]
Arenariumoside III (7)	54.1
Arenariumoside IV (8)	>100 (34.2)[b]
(2S)-Helichrysin (9)	>100 (39.4)[b]
(2R)-Helichrysin (10)	>100 (25.6)[b]
Naringenin 7-O-Glc (11)	>100 (4.6)[b]
5,7-Di-O-Glc-(2S)-naringenin (12)	>100 (48.7)[b]
5,7-Di-O-Glc-(2R)-naringenin (13)	>100 (30.0)[b]
Helicioside A (14)	>100 (33.3)[b]
(2R,3R)-Dihydrokaempferol 7-O-Glc (15)	>100 (1.3)[b]
Chalconaringenin 2′-O-Glc (16)	23.1
Chalconaringenin 2′,4′-di-O-Glc (17)	70.0
Apigenin 7-O-Glc (18)	62.7
Apigenin 7-O-GlcA methyl ester (19)	50.5
Apigenin 7-O-Glc-(1 → 6)-Glc (20)	32.0
Apigenin 7,4′-di-O-Glc (21)	>100 (39.6)[b]
Luteolin 7-O-Glc (22)	37.5
Luteolin 3′-O-Glc (23)	>100 (49.1)[b]
Scutellarein 7-O-Glc-(1 → 6)-Glc (24)	>100 (43.7)[b]
6-Hydroxyluteolin 7-O-Glc (25)	60.3
26	73.2
Kaempferol 7-O-Glc (27)	>100 (44.2)[b]
Kaempferol 3-O-Glc-(1 → 6)-Glc (28)	58.0
Kaempferol 3,7-di-O-Glc (29)	36.8
Kaempferol 3,4′-di-O-Glc (30)	88.6
31	85.2
Quercetin 3-O-Glc (32)	56.6
Rutin (33)	>100 (17.2)[b]
Quercetin 3,3′-di-O-Glc (34)	73.9
Aureusidin 6-O-Glc (35)	24.3
Alogliptin	0.0018
Diprotin A	2.3

[a] Each value represents the mean of 2–4 experiments

[b] Values in parentheses present inhibition % at 100 μM

strong inhibitory activity. In order to examine the inhibition type of DPP-IV by 16 and 35, the kinetic analysis was examined. Analysis of the Lineweaver-Burk plots indicated that the DPP-IV inhibition by 16 and 35 was of mixed type (Fig. 4).

In conclusion, a methanol extract of the flowers of *H. arenarium* was found to inhibit blood glucose elevation in
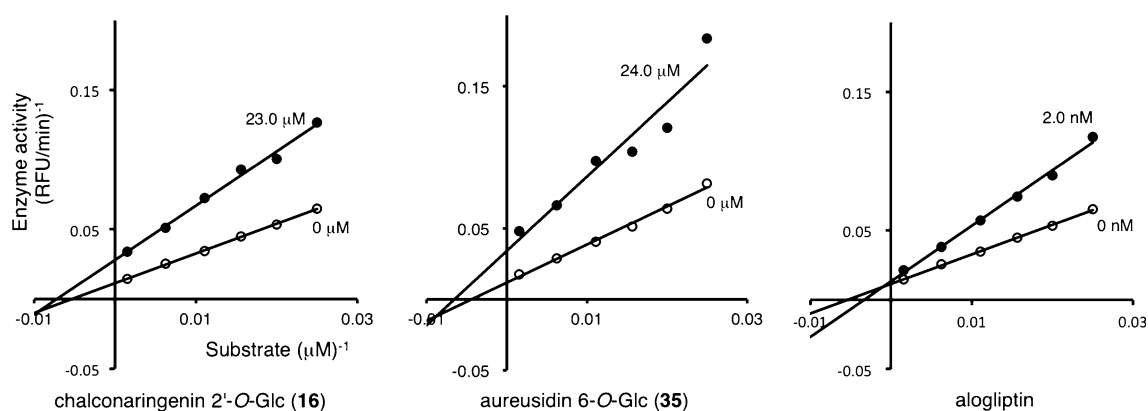
Fig. 4 Lineweaver-Burk plots of the inhibition of human recombinant DPP-IV activities by **16** and **35**

sucrose-loaded mice. The mode of action for the antihyperglycemic effect of the extract could be attributed to the observed inhibition of DPP-IV. Three new dimeric dihydrochalcone glycosides arenariumoside V–VII (**2–4**) together with 32 flavonoids were isolated using bioassay-guided fractionation. Compounds **2–4**, **7**, **16–20**, **22**, **25–32**, **34**, and **35** were able to inhibit DPP-IV enzymatic activity at IC_{50} ranging from 23.1 to 88.6 μM. Among the active constituents, chalconaringenin 2′-O-β-D-glucopyranoside (**16**, IC_{50} = 23.1 μM) and aureusidin 6-O-β-D-glucopyranoside (**35**, 24.3 μM) were found to be the most potent, and analysis of Lineweaver-Burk plots showed that they act through mixed competitive and non-competitive inhibition of the enzymes. Thus, these flavonoid constituents from *H. arenarium* may be useful agents for the prevention or treatment of type 2 diabetes.

Materials and methods

General

The following instruments were used to obtain spectroscopic data: specific rotations, Horiba SEPA-300 digital polarimeter (l = 5 cm); UV spectra, Shimadzu UV-1600 spectrometer; IR spectra, Shimadzu FTIR-8100 spectrometer; FAB-MS and high-resolution MS, JEOL JMS-SX 102A mass spectrometer; ^{1}H-NMR spectra, JEOL JNM-LA500 (500 MHz) and EX-270 (270 MHz) spectrometers; ^{13}C-NMR spectra, JEOL JNM-LA500 (125 MHz) and EX-270 (68 MHz) spectrometers in CD_3OD at room temperature or pyridine-d_5 at 40 °C with tetramethylsilane (TMS) as an internal standard; HPLC detector, Shimadzu RID-10A refractive index and SPD-10Avp UV–VIS detectors; HPLC column, Cosmosil 5C$_{18}$-MS-II (Nacalai Tesque Inc., Kyoto, Japan) and Wakopak Navi C30-5 (Wako Pure Chemical Industries, Ltd., Osaka, Japan)

(250 × 4.6 mm i.d. and 250 × 20 mm i.d. for analytical and preparative purposes, respectively).

The following experimental conditions were used for column chromatography (CC): highly porous synthetic resin, Diaion HP-20 (Mitsubishi Chemical Co., Tokyo, Japan); ordinary-phase silica gel CC, silica gel 60 N (Kanto Chemical Co., Tokyo, Japan; 63–210 mesh, spherical, neutral); reverse-phase ODS CC, Chromatorex ODS DM1020T (Fuji Silysia Chemical Ltd., Aichi, Japan; 100–200 mesh); normal-phase TLC, pre-coated TLC plates with silica gel 60F$_{254}$ (Merck, Darmstadt, Germany; 0.25 mm); reversed-phase TLC, pre-coated TLC plates with silica gel RP-18 F$_{254S}$ (Merck, 0.25 mm); reversed-phase HPTLC, pre-coated TLC plates with silica gel RP-18 WF$_{254S}$ (Merck, 0.25 mm). Detection was achieved by spraying with 1 % Ce(SO$_4$)$_2$–10 % aqueous H$_2$SO$_4$, followed by heating.

Plant material

This item was described in a previous report [4].

Extraction and isolation

The dried flowers of *H. arenarium* (3.0 kg) were extracted under reflux with methanol three times for 3 h. Evaporation of the solvent under reduced pressure provided a methanolic extract (593.8 g, 19.8 %). This methanolic extract (543.8 g) was partitioned with an EtOAc–H$_2$O (1:1, v/v) mixture, and removal of the solvents in vacuo yielded an EtOAc-soluble fraction (210.0 g, 7.6 %) and an aqueous phase. The aqueous phase was subjected to Diaion HP-20 CC (3.0 kg, H$_2$O → MeOH) to give H$_2$O-eluted (237.2 g, 8.6 %) and MeOH-eluted (88.6 g, 3.2 %) fractions, respectively.

The MeOH-eluted fraction (68.6 g) was subjected to normal-phase silica gel CC [2.5 kg, CHCl$_3$–MeOH–H$_2$O

(20:3:1 → 10:3:1 → 7:3:1, lower layer → 6:4:1, v/v/ v) → MeOH] to give 12 fractions [Fr. 1 (0.85 g), Fr. 2 (1.20 g), Fr. 3 (0.90 g), Fr. 4 (1.80 g), Fr. 5 (6.40 g), Fr. 6 (11.00 g), Fr. 7 (5.40 g), Fr. 8 (4.00 g), Fr. 9 (7.10 g), Fr. 10 (5.80 g), Fr. 11 (6.10 g), and Fr. 12 (17.10 g)], as reported previously [4–6]. Fraction 11 (5.0 g) was subjected to reversed-phase ODS CC [300 g, MeOH–H$_2$O (10:90 → 60:40, v/v) → MeOH] to afford 13 fractions [Fr. 11-1 (140.0 mg), Fr. 11-2 (180.0 mg), Fr. 11-3 (200.0 mg), Fr. 11-4 (130.0 mg), Fr. 11-5 (340.0 mg), Fr. 11-6 (180.0 mg), Fr. 11-7 (310.0 mg), Fr. 11-8 (310.0 mg), Fr. 11-9 (590.0 mg), Fr. 11-10 (255.0 mg), Fr. 11-11 (394.0 mg), Fr. 11-12 (470 0 mg), and Fr. 11-13 (498 mg)]. Fraction 11-9 (590.0 mg) was further purified by HPLC [Cosmosil 5C$_{18}$-MS-II, MeOH–H$_2$O (30:70, v/v) and Wakopak Navi C30-5, MeOH–H$_2$O (45:55, v/v)] to give arenariumoside VI (3, 41.0 mg, 0.010 %) together with arenariumoside III (18.4 mg, 0.0046 %), 6-hydroxyluteolin 7-O-β-D-glucopyranoside (25, 4.0 mg, 0.0010 %), kaempferol 3,4′-di-O-β-D-glucopyranoside (30, 44.7 mg, 0.011 %), and quercetin 3,3′-di-O-β-D-glucopyranoside (34, 6.0 mg, 0.0015 %), as reported previously [4]. Fraction 11-10 (255.0 mg) was purified by HPLC [Wakopak Navi C30-5, MeOH–H$_2$O (45:55, v/v)] to give arenariumoside VIII (4, 70.0 mg, 0.018 %). Fraction 12 (17.10 g) was subjected to reversed-phase ODS CC [500 g, MeOH–H$_2$O (10:90 → 40:60, v/v) → MeOH] to afford 11 fractions {Fr. 12-1 (1.10 g), Fr. 12-2 (1.50 g), Fr. 12-3 (1.30 g), Fr. 12-4 (0.67 g), Fr. 12-5 (0.46 g), Fr. 12-6 (0.40 g), Fr. 12-7 [= atomoroside A (1, 4055.0 mg, 1.014 %)] [17], Fr. 12-8 (576.0 mg), Fr. 12-9 (0.74 g), Fr. 12-10 (0.90 g), and Fr. 12-11 (2.97 g)}. Fraction 12-8 (576.0 mg) was separated by HPLC [Wakopak Navi C30-5, MeOH–H$_2$O (30:70, v/v)] to give 1 (250.0 mg, 0.062 %). Fraction 12-9 (740.0 mg) was separated by HPLC [Wakopak Navi C30-5, MeOH–H$_2$O (35:65, v/v)] to give 1 (60.0 mg, 0.015 %). Fraction 12-10 (900.0 mg) was separated by HPLC [Wakopak Navi C30-5, MeOH–H$_2$O (45:55, v/v)] to give arenariumoside V (2, 12.0 mg, 0.0030 %) together with everlastoside L (6.9 mg, 0.0018 %), as reported previously [4].

The EtOAc-soluble fraction (18.3 g) was subjected to normal-phase silica gel CC [550 g, hexane–EtOAc (5:1 → 2:1 → 1:1, v/v) → EtOAc → MeOH] to give 11 fractions [Fr. 1 (0.27 g), Fr. 2 (9.56 g), Fr. 3 (0.43 g), Fr. 4 (0.22 g), Fr. 5 (0.31 g), Fr. 6 (0.56 g), Fr. 7 (0.93 g), Fr. 8 (1.05 g), Fr. 9 (0.72 g), Fr. 10 (0.65 g), and Fr. 11 (11.40 g)]. Fraction 11 (11.40 g) was subjected to reversed-phase ODS CC [350 g, MeOH–H$_2$O (30:70 → 50:50 → 70:30, v/v) → MeOH → acetone] to afford 12 fractions [Fr. 11-1 (419.0 mg), Fr. 11-2 (265.0 mg), Fr. 11-3 (714.0 mg), Fr. 11-4 (435.0 mg), Fr. 11-5 (2.715 g), Fr. 11-6 (277.0 mg), Fr. 11-7 (116.0 mg),

Fr. 11-8 (2.479 g), Fr. 11-9 (241.0 mg), Fr. 11-10 (182.0 mg), Fr. 11-11 (1.033 g), and Fr. 11-12 (813.0 mg)]. Fraction 11-5 (500.0 mg) was further purified by HPLC [Cosmosil 5C$_{18}$-MS-II, MeOH–1 % aqueous AcOH (30:70, v/v)] to give (2R)-helichrysin A (9, 52.4 mg, 0.12 %) and (2S)-helichrysin A (10, 16.3 mg, 0.037 %). Fraction 11-8 (500.0 mg) was further purified by HPLC [Cosmosil 5C$_{18}$-MS-II, MeOH–1 % aqueous AcOH (40:60, v/v)] to give chalconeringenin 2′-O-β-D-glucopyranoside (16, 55.2 mg, 0.11 %), apigenin 7-O-β-D-glucopyranoside (18, 22.1 mg, 0.045 %), kaempferol 7-O-β-D-glucopyranoside (27, 190.3 mg, 0.39 %), and quercetin 3-O-β-D-glucopyranoside (32, 13.2 mg, 0.027 %). These isolates from the EtOAc-soluble fraction (9, 10, 16, 18, 27, and 32) were unambiguously identified by comparison of their physical and spectral data with those of authentic samples [4].

Arenariumoside V (2)

Yellowish amorphous powder, $[\alpha]_D^{27}$ +32.1 (c 0.65, MeOH); UV [MeOH, nm (log ε)]: 224 (3.61), 289 (3.43); IR (KBr) v_{max}: 3568, 1619, 1509, 1458, 1074 cm^{-1}; ^{1}H and ^{13}C NMR: given in Table 4; positive-ion FABMS m/z: 891 [M+Na]$^+$; HRFABMS m/z: 891.2319 [M+Na]$^+$ (calcd for C$_{42}$H$_{44}$O$_{20}$Na, 891.2324).

Arenariumoside VI (3)

Yellowish amorphous powder, $[\alpha]_D^{26}$ −16.7 (c 0.20, MeOH); UV [MeOH, nm (log ε)]: 224 (3.62), 298 (3.42); IR (KBr) v_{max}: 3590, 1620, 1509, 1458, 1075 cm^{-1}; ^{1}H and ^{13}C NMR: given in Table 4; positive-ion FABMS m/z: 891 [M + Na]$^+$; HRFABMS m/z: 891.2332 [M+Na]$^+$ (calcd for C$_{42}$H$_{44}$O$_{20}$Na, 891.2324).

Arenariumoside VII (4)

Yellowish amorphous powder, $[\alpha]_D^{27}$ +6.0 (c 0.28, MeOH); UV [MeOH, nm (log ε)]: 223 (3.70), 287 (3.53); IR (KBr) v_{max}: 3568, 1638, 1509, 1458, 1073 cm^{-1}; ^{1}H and ^{13}C NMR: given in Table 4; positive-ion FABMS m/z: 891 [M + Na]$^+$; HRFABMS m/z: 891.2327 [M+Na]$^+$ (calcd for C$_{42}$H$_{44}$O$_{20}$Na, 891.2324).

Acid hydrolysis of 1–4

A solution of 1–4 (each 2.0 mg) in 1 M HCl (1.0 ml) was stirred at 80 °C for 1 h. After being cooled, the reaction mixture was neutralized with Amberlite IRA-400 (OH$^-$ form), and the resin was removed by filtration. After removal of the solvent from the filtrate under reduced pressure, the residue was separated using a Sep-Pak C18 cartridge column

($H_2O \rightarrow MeOH$). The H_2O-eluted fraction was subjected to HPLC analysis under the following conditions: HPLC column, Kaseisorb LC NH_2-60-5, 4.6 mm i.d. × 250 mm (Tokyo Kasei Co., Ltd., Tokyo, Japan); detection, optical rotation [Shodex OR-2 (Showa Denko Co., Ltd., Tokyo, Japan); mobile phase, CH_3CN-H_2O (85:15, v/v); flow rate 0.8 ml/min]. Identification of D-glucose from **1–4** present in the H_2O-eluted fraction was carried out by comparing the retention time and the optical rotation with the standard [t_R: 13.9 min (positive optical rotation)] [21, 22].

In vivo assay

Animals

Male ddY mice (6 weeks old) were purchased from Kiwa Laboratory Animal Co., Ltd., Wakayama, Japan. The animals were housed at a constant temperature of 23 ± 2 °C and were then fed a standard laboratory chow (MF, Oriental Yeast Co., Ltd., Tokyo, Japan). The animals were fasted for 20–24 h prior to the beginning of the experiment, but were allowed free access to tap water. All of the experiments were performed on conscious mice unless otherwise noted. The experimental protocol was approved by the Experimental Animal Research Committee at Kinki University.

Effects on plasma glucose levels in sucrose-loaded mice

The experiments were performed according to the method as described in our previous reports with a slight modification [31, 32]. Thus, a mixture of each test sample and sucrose (2 g/kg) suspended in 5 % (w/v) acacia solution (20 ml/kg) was administered orally to fasted mice (body weight 24–27 g). Blood samples (ca. 0.1 ml) were collected from the infraorbital venous plexus under ether anesthesia 0.5, 1, and 2 h after the oral administration. The collected blood was immediately mixed with heparin sodium (5 units/tube). After centrifugation of the blood samples, the plasma glucose level was determined enzymatically by the Wako Glucose CII test (Wako Pure Chemical Industries Ltd., Osaka, Japan) according to the manufacturer's instructions. The intestinal α-glucosidase inhibitor acarbose was used as a reference compound [31].

In vitro assay

Inhibitory effects on rat intestinal α-glucosidases

The experiments were performed as described previously [33–35]. Briefly, the assay was performed in 96-well microplates. Rat small intestinal brush border membrane vesicles were prepared, and a suspension of these in 0.1 M maleate buffer (pH 6.0) was used to determine the activities of maltase and sucrase. A test sample was dissolved in dimethyl sulfoxide (DMSO), and the resulting solution was diluted with 0.1 M maleate buffer to prepare the test sample solution (concentration of DMSO: 10 %). A substrate solution in the maleate buffer (maltose or sucrose: 74 mM, 50 μl), the test sample solution (25 μl), and the enzyme solution (25 μl) were mixed at 37 °C for 30 min and then immediately heated by boiling water for 2 min to stop the reaction. The glucose concentrations were determined by a glucose-oxidase method. The final concentration of DMSO in the test solution was 2.5 %, and no influence of DMSO on the inhibitory activity was detected. The IC_{50} was determined graphically ($N = 2$–4). The intestinal α-glucosidase inhibitors acarbose ($IC_{50} = 1.7$ and 1.5 μM against maltase and sucrase, respectively) and salacinol ($IC_{50} = 6.0$ and 1.3 μM) were used as reference compounds [33–35].

Inhibitory effect on human recombinant DPP-IV

The experiment was performed according to the method described in our previous reports with a slight modification [16]. Briefly, the assay was performed in 96-well half area white microplates (flat bottom). Pre-incubation of 15 μl of DPP-IV enzyme (from human recombinant; 17.3 mU/ml) or a blank buffer (50 mM tris HCl buffer, pH 7.5) with 35 μl of sample or control was incubated at room temperature (25 °C) for 10 min. Fifty microliters of H-Gly-Pro-7-amino-4-methylcoumarin (Gly-Pro-AMC) substrate (4 mg/ml) was added, and the mixture was incubated at 25 °C for 30 min. During the incubation, the fluorescence was measured using a fluorescence microplate reader (SH-9000, CORONA) at an excitation wavelength of 380 nm and an emission wavelength of 460 nm. The final concentration of DMSO in the test solution was 1.0 %, and no influence of DMSO on the inhibitory activity was detected. The IC_{50} was determined graphically ($N = 2$–4). The DPP-IV inhibitors alogliptin ($IC_{50} = 18$ nM) and diprotin A (Ile-Pro-Ile, $IC_{50} = 2.3$ μM) were used as reference compounds.

For kinetic analysis of their inhibitory activity on human recombinant DPP-IV by chalcogenin 2′-O-β-D-glucopyranoside (**16**) and aureusidin 6-O-β-D-glucopyranoside (**35**), the enzyme (final concentration: 0.42 mU/ml) and each test compound [**16** (23 μM), **35** (24 μM), or alogliptin (2 nM)] were incubated with increasing concentrations of the substrate (40–640 μM). A typical type of competitive inhibitior, alogliptin ($K_i = 2.3$ nM), was used as a reference.

Statistical analysis

Values were expressed as mean ± SEM. For statistical analysis, one-way analysis of variance followed by Dunnett's test was used.

References

1. Czinner E, Hagymási K, Blázovics A, Kéry Á, Szöke É, Lemberkovics É (2000) In vitro antioxidant properties of *Helichrysum arenarium* (L.) Moench. J Ethnopharmacol 73:437–443

2. Gradinaru AC, Silion M, Trifan A, Miron A, Aprotosoaie AC (2014) *Helichrysum arenarium* subsp. *arenarium*: phenolic composition and antibacterial activity against lower respiratory tract pathogens. Nat Prod Res 28:2076–2080

3. Vrkoc J, Dolejs L, Sedmera P, Vasickova S, Sorm F (1971) Structure of arenol and homoarenol, α-pyrone derivatives from *Helichrysum arenarium*. Therahedron Lett 3:247–250

4. Morikawa T, Wang L-B, Nakamura S, Ninomiya K, Yokoyama E, Matsuda H, Muraoka O, Wu L-J, Yoshikawa M (2009) Medicinal flowers. XXVII. new flavanone and chalcone glycosides, arenariumosides I, II, III, and IV, and tumor necrosis factor-α inhibitors from everlasting, flowers of *Helichrysum arenarium*. Chem Pharm Bull 57:361–367

5. Morikawa T, Wang L-B, Ninomiya K, Nakamura S, Matsuda H, Muraoka O, Wu L-J, Yoshikawa M (2009) Medicinal flowers. XXX. Eight new glycosides, everlastosides F–M, from the flowers of *Helichrysum arenarium*. Chem Pharm Bull 57:853–859

6. Wang L-B, Morikawa T, Nakamura S, Ninomiya K, Matsuda H, Muraoka O, Wu L-J, Yoshikawa M (2009) Medicinal flowers. XXVIII. structures of five new glycosides, everlastosides A, B, C, D, and E, from the flowers of *Helichrysum arenarium*. Heterocycles 78:1235–1242

7. Wang L-B, Wang J, Gan C, Wu L-J, Liu F (2011) Chemical constituents in fraction of lipid-lowering of Helichrysi arenarii flos. Shenyang Yaoke Daxue Xuebao 28(868–870):916

8. Wang L-B, Liu F, Gan C, Dong N, Hou Y, Wang C (2012) Isolation and identification of chemical constituents in the lipid-lowering fraction of flos *Helichrysum arenarium* (II). Shenyang Yaoke Daxue Xuebao 29(109–112):125

9. Wang L-B, Wang J-W, Wang C, Sun S-C, Xu B, Wu L-J (2012) Chemical constituents in the lipid-lowering fraction of flos *Helichrysum arenarium* (III). Zhongguo Yaowu Huaxue Zazhi 22(220–222):226

10. Vrkoc J, Ubik K, Sedmera P (1973) Phenolic extractives from the achenes of *Helichrysum arenarium*. Phytochemistry 12:2062

11. Vrkoc J, Dolejs L, Budesinsky M (1975) Methylene-bis-2*H*-pyran-2-ones and phenolic constituents from the root of *Helichrysum arenarium*. Phytochemistry 14:1383–1384

12. Vrkoc J, Budesinsky M, Dolejs L, Vasickova S (1975) Arenophthalide A, a new phthalide glycoside from *Helichrysum arenarium* roots. Phytochemistry 14:1845–1848

13. Mericli AH, Damadyan B, Cubukcu B (1986) Flavonoids of Turkish *Helichrysum arenarium* (L.) Moench (Asteraceae). Sci Pharm 54:363–365

14. Ahrén B (2008) Emerging dipeptidyl peptidase-4 inhibitors for the treatment of diabetes. Expert Opin Emerg Drugs 13:593–607

15. Mulakayala N, Reddy CHU, Iqbal J, Pal M (2010) Synthesis of dipeptidyl peptidase-4 inhibitors: a brief overview. Tetrahedron 66:4919–4938

16. Hussein GME, Matsuda H, Nakamura S, Hamao M, Akiyama T, Tamura K, Yoshikawa M (2011) Mate tea (*Ilex paraguariensis*) promotes satiety and body weight lowering in mice: involvement of glucagon-like peptide-1. Biol Pharm Bull 34:1849–1855

17. Aljančić IS, Vučković I, Jadranin M, Pešić M, Đorđević I, Podolski-Renić A, Stojković S, Menković N, Vajs VE, Milosavljević SM (2014) Two structurally distinct chalcone dimers from *Helichrysum zivojinii* and their activities in cancer cell lines. Phytochemistry 98:190–196

18. Montaudo G, Caccamese S (1973) Structure and conformation of chalcone photodimers and related compounds. J Org Chem 38:710–716

19. Montaudo G, Caccamese S, Librando V (1974) Photodimers of cinnamic acid and related compounds. A stereochemical study by NMR. Org Magn Res 6:534–536

20. Nozaki H, Hayashi K, Kido M, Kakumoto K, Ikeda S, Matsuura N, Tani H, Takaoka D, Iinuma M, Akao Y (2007) Pauferrol A, a novel chalcone trimer with a cyclobutane ring from *Caesalpinia ferrea* mart exhibiting DNA topoisomerase II inhibition and apoptosis-inducing activity. Tetrahedron Lett 48:8290–8292

21. Morikawa T, Ninomiya K, Miyake S, Miki Y, Okamoto M, Yoshikawa M, Muraoka O (2013) Flavonol glycosides with lipid accumulation inhibitory activity and simultaneous quantitative analysis of 15 polyphenols and caffeine in the flower buds of *Camellia sinensis* from different regions by LCMS. Food Chem 140:353–360

22. Morikawa T, Ninomiya K, Imura K, Yamaguchi T, Akagi Y, Yoshikawa M, Hayakawa T, Muraoka O (2014) Hepatoprotectie triterpenes from traditional Tibetan medicine *Potentilla anserina*. Phytochemistry 102:169–181

23. Drewes SE, Hudson NA (1983) Brackenin, a dimeric dihydrochalcone from *Brackenridgea zanguebarica*. Phytochemistry 22:2823–2825

24. Masaoud M, Ripperger H, Himmelreich U, Adam G (1995) Cinnabarone, a biflavonoid from dragon's blood of *Dracaena cinnabari*. Phytochemistry 38:751–753

25. Seidel V, Bailleul F, Waterman PG (2000) (*Rel*)-1β,2α-di-(2,4-dihydroxy-6-methoxybenzoyl)-3β,4α-di-(4-methoxyphenyl)-cyclobutane and other flavonoids from the aerial parts of *Goniothalamus gardneri* and *Goniothalamus thwaitesii*. Phytochemistry 55:439–446

26. Li Y-S, Matsunaga K, Kato R, Ohizumi Y (2001) Verbenachalcone, a novel dimeric dihydrochalcone with potentiating activity on nerve growth factor-action from *Verbena littoralis*. J Nat Prod 64:806–808

27. Patil AD, Freyer AJ, Killmer L, Offen P, Taylor PB, Votta BJ, Johnson RK (2002) A new dimeric dihydrochalcone and a new prenylated flavone from the bud covers of *Artocarpus altilis*: potent inhibitors of cathepsin K. J Nat Prod 65:624–627

28. Katerere DR, Gray AI, Kennedy AR, Nash RJ, Waigh RD (2004) Cyclobutanes from *Combretum albopunctatum*. Phytochemistry 65:433–438

29. Kamara BI, Manong DTL, Brandt EV (2005) Isolation and synthesis of a dimeric dihydrochalcone from *Agapanthus africanus*. Phytochemistry 66:1126–1132

30. Kumar M, Rawat P, Rahuja N, Srivastava AK, Maurya R (2009) Antihyperglycemic activity of phenylpropanoyl esters of catechol glycoside and its dimers from *Dodecadenia grandiflora*. Phytochemistry 70:1448–1455

31. Morikawa T, Chaipech S, Matsuda H, Hamao M, Umeda Y, Sato H, Tamura H, Kon'i H, Ninomiya K, Yoshikawa M, Pongpiriyadacha Y, Hayakawa T, Muraoka O (2012) Antidiabetogenic oligostilbenoids and 3-ethyl-4-phenyl-3,4-dihydroisocoumarins from the bark of *Shorea roxburghii*. Bioorg Med Chem 20:832–840

32. Morikawa T, Ninomiya K, Imamura M, Akaki J, Fujikura S, Pan Y, Yuan D, Yoshikawa M, Jia X, Li Z, Muraoka O (2014) Acylated phenylethanoid glycosides, echinacoside and acteoside from *Cistanche tubulosa*, improve glucose tolerance in mice. J Nat Med 68:561–566

33. Muraoka O, Morikawa T, Miyake S, Akaki J, Ninomiya K, Yoshikawa M (2010) Quantitative determination of potent α-glucosidase inhibitors, salacinol and kotalanol, in *Salacia* species using liquid chromatography-mass spectrometry. J Pharm Biomed Anal 52:770–773

34. Muraoka O, Morikawa T, Miyake S, Akaki J, Ninomiya K, Pongpiriyadacha Y, Yoshikawa M (2011) Quantitative analysis of neosalacinol and neokotalanol, another two potent α-glucosidase inhibitors from *Salacia* species, by LC-MS with ion pair chromatography. J Nat Med 65:142–148

35. Akaki J, Morikawa T, Miyake S, Ninomiya K, Okada M, Tanabe G, Pongpiriyadacha Y, Yoshikawa M, Muraoka O (2014) Evaluation of *Salacia* species as anti-diabetic natural resources based on quantitative analysis of eight sulphonium constituents: a new class of α-glucosidase inhibitors. Phytochem Anal 25:544–550